PHYSICAL REVIEW B VOLUME 23, NUMBER 6 15 MARCH 1981

Umklapp electron-electron scattering and the low-temperature electrical resistivity of the alkali metals

A. H. MacDonald and Roger Taylor
Division of Physics, National Research Council of Canada, Ottawa K1A OR6, Canada

D. J. W. Geldart
Department of Physics, Dalhousie University, Halifax B3H 3J5, Canada

(Received 11 August 1980)

The umklapp fraction, Δ, for electron-electron scattering in the alkali metals has been calculated using first-principles pseudopotentials. Both Coulomb scattering and phonon-exchange scattering have been included. For a given pseudopotential and a given approximation to the effective electron-electron interaction, our results for the Coulomb scattering contribution to Δ are up to a factor of ~ 100 smaller than those of an earlier calculation. The sources of this discrepancy have been analyzed. On the basis of these calculations we suggest that the scattering amplitude for umklapp electron-electron scattering in the alkali metals is dominated by the phonon-exchange contribution. The improved treatment of the Coulomb contribution to the scattering amplitude and the inclusion of the phonon-exchange contribution combine to yield a coefficient of T^2 in the low-T electrical resistivity which is larger than earlier theoretical values for Li and Na, about the same size for K, and smaller for Rb and Cs.

I. INTRODUCTION

It has long been recognized[1] that the ideal electrical resistivity of metals, $\rho_i(T)$, should be dominated at sufficiently low temperatures by a term proportional to T^2 due to electron-electron scattering:

$$\rho_{ee}(T)=A_{ee}T^2 . \tag{1}$$

The existence of such a term in $\rho_i(T)$ in transition metals, where ρ_{ee} frequently dominates ρ_i up to ~20 K, is well established.[2] For simple metals the situation has been less clear.[3,4] However, recent advances in high-precision techniques have made possible convincing observations of T^2 variations in the electrical resistivities of Al (Refs. 5, 6), Cu (Ref. 7), and Ag (Ref. 8). Similar variations have been reported for K but in this case the experimental situation is not yet completely clear.[9-11] It has usually been assumed that only Coulomb electron-electron scattering need be considered in evaluating A_{ee} (Ref. 12); in this article we report calculations of A_{ee} for the alkali metals which include both Coulomb and phonon-exchange scattering mechanisms. We find that, even though the Coulomb interaction dominates for normal scattering events, A_{ee} is determined almost solely by the phonon-exchange scattering process.

The work presented here is in part a refinement of earlier work by Lawrence and Wilkins.[3] These authors have presented an accurate but approximate solution of the appropriate Boltzmann equation which expresses A_{ee} in terms of a factor which is proportional to the electron-electron scattering rate on the Fermi surface and a factor Δ which they call the "fractional umklapp scattering." Δ is a measure of the average depletion of current in an electron-electron scattering event. Lawrence and Wilkins have evaluated Δ by assuming that the quasiparticle wave functions for Fermi-surface electrons can be determined by solving a Schrödinger equation with a local pseudopotential and that the transition probabilities for electron-electron scattering events can be approximated by treating a Thomas-Fermi screened Coulomb interaction in the Born approximation.

In Sec. II we adopt these approximations and, at the expense of obtaining results numerically rather than analytically, are able to evaluate Δ without further significant approximations. For a given pseudopotential our results for Δ are up to a factor of ~100 smaller than those obtained by Lawrence and Wilkins, and the sources of this discrepancy are discussed. In Sec. III we attempt to improve on these calculations by using reliable but highly nonlocal first-principles pseudopotentials (see below). In addition we consider many-body effects on the electron-ion interaction and their influence on Δ. In particular a frequently quoted conclusion of previous workers,[13] that the scattering potential determining the shape of the Fermi surface is identical with that appearing in the electron-phonon scattering amplitude, is examined. Finally in Sec. IV we combine the results for Δ obtained in Sec. III with a recently suggested approximation for the electron-electron scattering[14] rate in order to obtain A_{ee}. The discussion in Secs. II–IV is all based on the usual assumption that phonon-exchange scattering process can be ignored in evaluating A_{ee}. In Sec. V

this latter process is included in evaluating A_{ee} and is found to be totally dominant. The values obtained for A_{ee} are compared with available experimental data and predictions are made concerning the observability of electron-electron scattering coefficients in the electrical resistivities of all alkali metals. Finally, in Sec. VI we present our conclusions.

II. THE UMKLAPP FRACTION IN THE LOCAL PSEUDOPOTENTIAL APPROXIMATION

According to Lawrence and Wilkins[3]

$$A_{ee}=\frac{2\pi^4 m^*\Delta}{k_F^3 e^2 \tau_0 T^2} \tag{2}$$

for simple metals in the impurity-dominated limit. In Eq. (2), τ_0^{-1} is proportional to the electron- electron scattering rate at the Fermi surface and

$$\Delta \equiv \left(\int\prod_{i=1}^{4} d\vec{k}_i\,\delta(\epsilon_{\vec{k}_i}-\epsilon_F)\,\omega(\vec{k}_1,\vec{k}_2;\vec{k}_3,\vec{k}_4)\,|\vec{V}_1+\vec{V}_2-\vec{V}_3-\vec{V}_4|^2\right)\left[4\left(\int\prod_{i=1}^{4} d\vec{k}_i\,\delta(\epsilon_{\vec{k}_i}-\epsilon_F)\,\omega(\vec{k}_1,\vec{k}_2;\vec{k}_3,\vec{k}_4)\,|\vec{V}_1|^2\right)\right]^{-1}, \tag{3}$$

where $\vec{V}_i$ is the quasiparticle group velocity at $\vec{k}_i$ and $\omega(\vec{k}_1,\vec{k}_2;\vec{k}_3,\vec{k}_4)$ is the average over spin states of the transition probabilities for initial states $\vec{k}_1$ and $\vec{k}_2$ and final states $\vec{k}_3$ and $\vec{k}_4$. Here we will follow Lawrence and Wilkins in writing

$$\omega(\vec{k}_1,\vec{k}_2,\vec{k}_3,\vec{k}_4)=\frac{2\pi}{\hbar}\left(|\langle\vec{k}_3,\vec{k}_4|V^{\mathrm{TF}}|\vec{k}_1,\vec{k}_2\rangle|^2+\tfrac{1}{2}|\langle\vec{k}_3,\vec{k}_4|V^{\mathrm{TF}}|\vec{k}_1,\vec{k}_2\rangle-\langle\vec{k}_4,\vec{k}_3|V^{\mathrm{TF}}|\vec{k}_1,\vec{k}_2\rangle|^2\right), \tag{4}$$

where

$$V^{\mathrm{TF}}(\vec{r}-\vec{r}')=\frac{e^2\exp(-|\vec{r}-\vec{r}'|k_{\mathrm{TF}})}{|\vec{r}-\vec{r}'|} \tag{5}$$

is the Thomas-Fermi screened Coulomb interaction and $\{|\vec{k}_i\rangle\}$ are the quasiparticle wave functions. Note that we adopt this approximation in evaluating Δ, which is the ratio of two quantities averaged with respect to ω, but not in evaluating τ_0^{-1}. For the moment we also assume that the core-orthogonalization components of the wave function can be ignored in evaluating Eq. (1) so that

$$|\vec{k}\rangle=\frac{1}{\sqrt{\Omega}}\sum_i C_i(\vec{k})\exp[i(\vec{k}+\vec{G}_i)\cdot\vec{r}], \tag{6}$$

where

$$\sum_j[|\vec{k}+\vec{G}_j|^2\delta_{i,j}+V(|\vec{G}_i-\vec{G}_j|)]C_j(\vec{k})=\epsilon_{\vec{k}}C_i(\vec{k}) \tag{7}$$

and $V(|\vec{G}_i-\vec{G}_j|)$ are the Fourier components of a local pseudopotential. Atomic units with Ry for energy have been used and it is understood that the lowest eigenvalue and eigenfunction of Eq. (7) are the solutions of interest. From Eqs. (6) and (7) it follows that

$$V_{\vec{k}}=\nabla_{\vec{k}}\epsilon_{\vec{k}}=\sum_i |C_i(\vec{k})|^2 2(\vec{k}+\vec{G}_i) \tag{8}$$

while from Eqs. (5) and (7) it follows that

$$\langle\vec{k}_3,\vec{k}_4|V^{\mathrm{TF}}|\vec{k}_1,\vec{k}_2\rangle=\frac{1}{\Omega}\sum_i\delta_{\vec{k}_1+\vec{k}_2+\vec{G}_i,\vec{k}_3+\vec{k}_4}\sum_n\sum_{m,m'}\frac{4\pi e^2 C_n^*(\vec{k}_3)C_{n'}^*(\vec{k}_4)C_m(\vec{k}_1)C_{m'}(\vec{k}_2)}{|\vec{k}_3-\vec{k}_1+\vec{G}_n-\vec{G}_m|^2+k_{\mathrm{TF}}^2}, \tag{9}$$

where n' satisfies $\vec{G}_{n'}=\vec{G}_{m'}+\vec{G}_m-\vec{G}_n-\vec{G}_i$.

We note from Eq. (9) that $\omega(\vec{k}_1,\vec{k}_2;\vec{k}_3,\vec{k}_4)$ is nonzero only when $\vec{k}_1+\vec{k}_2+\vec{G}_i=\vec{k}_3+\vec{k}_4$ and $\vec{G}_i$ is some reciprocal-lattice vector. This is a consequence of the translational symmetry of the lattice and not an artifact of our simple approximation for ω. If in addition we approximate ϵ_k by k^2/m^* in evaluating Eq. (3), we need consider only integrals of the form

$$\langle F_i\rangle=\left(\frac{2}{k_F}\right)^4\int\left(\prod_{i=1}^{4} d\vec{k}_i\,\delta(k_i^2-k_F^2)\right)\times\delta(\vec{k}_1+\vec{k}_2+\vec{G}_i-\vec{k}_3-\vec{k}_4)\times\omega(\vec{k}_1,\vec{k}_2;\vec{k}_3,\vec{k}_4)F(\vec{k}_1,\vec{k}_2;\vec{k}_3,\vec{k}_4), \tag{10}$$

which can be accurately evaluated numerically (see Appendix). In terms of these integrals $\Delta=\sum_{i=1}^{4}\Delta_i$ where

$$\Delta_i = \sum_{j\in}^{i\text{th shell}} \langle|\vec{V}_1+\vec{V}_2-\vec{V}_3-\vec{V}_4|^2_j\rangle \Big/ \left(4 \sum_{j\in}^{\text{all shells}} \langle|\vec{V}_1|\rangle^2_j\right), \tag{11}$$

and as shown in the Appendix, in the case of the alkali metals $\langle F_i\rangle$ is nonzero only for reciprocal-lattice vectors contained in the first four shells. We have evaluated Δ from these equations for a number of local pseudopotentials for each of the alkali metals. The sums over reciprocal-lattice vectors were truncated after the 19 $\vec{G}$'s in the first three shells. A total of $\sim 2\times 10^4$ $\{\vec{k}_i\}$ points were used in calculating $\langle F_i\rangle$ and these numerical results were found to be well converged. The results of this calculation are listed in Table I and the pseudopotentials used are in Table II.

We discuss our results in terms of the approximate expression given by Lawrence and Wilkins, which for the alkali metals is

$$\Delta \sim 2.3 \left(\frac{V_{110}}{V_0}\right)^2, \tag{12}$$

where V_{110} is a Fourier component of the pseudopotential for the first shell of reciprocal-lattice vectors and $V_0 = -\frac{2}{3}\epsilon_F$ is the average value of the pseudopotential. This estimate is based on the expectation that $\Delta \sim \Delta_1$ and from Table I we note our results are in accord on this point. However, comparing Tables I and II we see that our result for Δ is on average a factor of ~25 smaller than what would be predicted by Eq. (12). Moreover, $\Delta_1/(V_{110}/V_0)^2$ was found to vary significantly from pseudopotential to pseudopotential and from metal to metal. Three possible sources of this variation come to mind. First of all, it is clear from Tables I and II that a nonzero value for V_{200}, especially if $|V_{200}| \gg |V_{110}|$, can have a significant impact on the value of Δ_1. Secondly, even with $V_{200}=0$, we see from Eq. (9) that Δ_1 can depend on r_s at constant (V_{110}/V_0) through the density dependence of the screening wave vector $(k_{TF}/k_F)^2 \sim 0.66 r_s$, where r_s is the usual conduction-electron density parameter. This rather weak dependence is illustrated in Fig. 1. Finally, while Δ_1 should be proportional to V_{110}^2 to leading order in the pseudopotential, it is possible that higher-order corrections are entering even for the relatively small V_{110} values of the alkali metals. As shown in Fig. 2 we find this to be so.

Because of the weak density dependence of $\Delta/(V_{110}/V_0)^2$ we can, however, give a result for Δ in the linear-response limit which is approximately valid over the entire alkali density regime.

TABLE I. Results for the fractional umklapp scattering Δ in the alkali metals. Δ_0 is the normal scattering contribution. Δ_1, Δ_2, and Δ_3 give the umklapp contributions. The pseudopotentials used are listed in Table II.

Metal	Potential	Δ_0	Δ_1	Δ_2	Δ_3	Δ
Li	RT	4×10^{-4}	1.8×10^{-3}	3×10^{-5}	8×10^{-9}	2.2×10^{-3}
Li	CH	6×10^{-4}	2.2×10^{-3}	1×10^{-5}	5×10^{-9}	2.8×10^{-3}
Li	HA	7×10^{-4}	2.8×10^{-3}	2×10^{-5}	2×10^{-8}	3.5×10^{-3}
Li	S	3×10^{-4}	1.9×10^{-3}	4×10^{-5}	1×10^{-8}	2.2×10^{-3}
Li	AL	6×10^{-4}	3.0×10^{-3}	6×10^{-5}	3×10^{-8}	3.7×10^{-3}
Na	RT	1×10^{-5}	3.8×10^{-4}	2×10^{-5}	2×10^{-10}	4.1×10^{-4}
Na	CH	3×10^{-6}	2.6×10^{-4}	3×10^{-8}	2×10^{-11}	2.6×10^{-4}
Na	HA	5×10^{-5}	9.1×10^{-4}	2×10^{-6}	2×10^{-10}	9.6×10^{-4}
Na	S	2×10^{-5}	6.2×10^{-4}	8×10^{-6}	4×10^{-10}	6.5×10^{-4}
Na	AL	2×10^{-6}	1.8×10^{-4}	1.2×10^{-5}	6×10^{-11}	1.9×10^{-4}
Na	A	9×10^{-6}	4.4×10^{-4}	8×10^{-8}	6×10^{-11}	4.4×10^{-4}
K	RT	2×10^{-8}	5.0×10^{-5}	1.6×10^{-5}	7×10^{-12}	6.6×10^{-5}
K	CH	7×10^{-7}	1.4×10^{-4}			1.4×10^{-4}
K	HA	4×10^{-8}	3.7×10^{-5}			3.7×10^{-5}
K	S	6×10^{-7}	1.2×10^{-4}			1.2×10^{-4}
K	AL	2×10^{-6}	3.3×10^{-4}			3.3×10^{-4}
K	A	9×10^{-5}	1.5×10^{-3}			1.6×10^{-3}
Rb	RT	1×10^{-3}	1.7×10^{-2}	3×10^{-4}	7×10^{-8}	1.8×10^{-2}
Rb	CH	2×10^{-4}	2.7×10^{-3}			2.9×10^{-3}
Rb	HA	3×10^{-5}	1.1×10^{-3}			1.1×10^{-3}
Rb	AL	1×10^{-4}				
Cs	RT	3×10^{-3}	3.5×10^{-2}			3.8×10^{-2}
Cs	CH	8×10^{-4}	6.7×10^{-3}			7.5×10^{-3}
Cs	HA	1×10^{-3}	1.1×10^{-2}			1.2×10^{-2}
Cs	AL	1×10^{-3}	1.1×10^{-2}			1.2×10^{-2}

TABLE II. Pseudopotentials used to obtain the results listed in Table I. For nonlocal pseudopotentials we have used the back-scattering matrix elements in these calculations. The pseudopotentials are given in units of $-2\epsilon_F/3$.

Metal	Potential	V_{110}	V_{200}	V_{211}	V_{220}	V_{310}
Li	RT [a]	0.323	0.253	0.114	0.016	−0.034
Li	CH [b]	0.325				
Li	HA [c]	0.428	0.269			
Li	S [d]	0.308	0.257			
Li	AL [e]	0.436	0.376			
Na	RT [f]	0.097	0.120	0.070	0.027	−0.002
Na	CH [b]	0.063				
Na	HA [c]	0.138	0.057			
Na	S [d]	0.113	0.088			
Na	AL [e]	0.057	0.094			
Na	A [g]	0.084				
K	RT [a]	−0.013	−0.087	−0.149	−0.154	−0.127
K	CH [b]	−0.038				
K	HA [c]	−0.019	−0.048			
K	S [d]	0.038	−0.019			
K	AL [e]	−0.048	−0.163			
K	A [g]	0.165				
Rb	RT [h]	−0.153	−0.268	−0.282	−0.214	−0.121
Rb	CH [b]	−0.143				
Rb	HA [c]	−0.088	−0.088			
Rb	AL [e]	−0.121	−0.198			
Cs	RT [h]	−0.277	−0.357	−0.223	−0.054	0.053
Cs	CH [b]	−0.21				
Cs	HA [c]	−0.23	−0.13			
Cs	AL [e]	−0.21	−0.26			

[a] Reference 30.
[b] Reference 41.
[c] Reference 42.
[d] Reference 43.
[e] Reference 44.
[f] Reference 31.
[g] Reference 45.
[h] Reference 34.

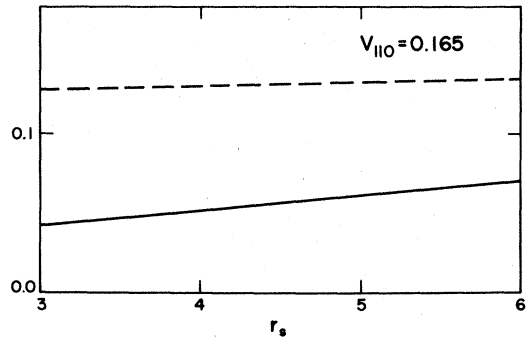

FIG. 1. Contributions to Δ from zeroth and first shells of reciprocal-lattice vectors as a function of r_s for a local pseudopotential with $V_{\vec{G}} \neq 0$ only for the first shell of reciprocal-lattice vectors. The calculation was performed for $V_{110}/V_0 = 0.165$ corresponding to the Ashcroft pseudopotential in K. The dashed curve is $\Delta_0/(V_{110}/V_0)^4$ while the solid curve is $\Delta_1/(V_{110}/V_0)^2$. The low-density ($r_s \to \infty$) limits are $\Delta_0/(V_{110}/V_0)^4 = 0.14$ and $\Delta_1/(V_{110}/V_0)^2 = 0.16$.

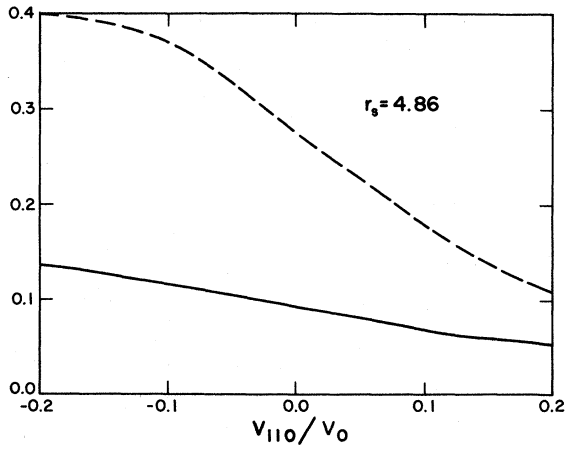

FIG. 2. As in Fig. 1 but as a function of V_{110}/V_0 for $r_s = 4.86$ corresponding to K. Note that Δ tends to be larger at a given (V_{110}/V_0) magnitude if V_{110}/E_F is positive.

From Fig. 2,

$$\Delta \sim 0.1 \left(\frac{V_{110}}{V_0}\right)^2 \left[1 + O\left(\frac{V_{110}}{V_0}\right)\right] . \tag{13}$$

The coefficients of V_{110}^2 in Eqs. (12) and (13) differ by a factor of ~25 and we have attempted to identify the sources of this discrepancy. First of all we note that in evaluating $\langle |\vec{V}_1 + \vec{V}_2 - \vec{V}_3 - \vec{V}_4|_j^2 \rangle$, Lawrence and Wilkins have included only $\vec{G}_i = 0$ and $\vec{G}_i = \pm \vec{G}_j$ in the reciprocal-lattice sums. When we make the corresponding reduction in the number of plane waves in the pseudo-wave-function expansion, we find our estimate of Δ increases by a factor of ~3. This increase can be understood by examining Eq. (9). A typical term appearing in the sum of Eq. (9) when evaluating $\langle F_j \rangle$ is

$$\frac{C_0^*(\vec{k}_3) C_j^*(\vec{k}_4) C_0(\vec{k}_1) C_0(\vec{k}_2)}{|\vec{k}_3 - \vec{k}_1|^2 + k_{TF}^2} \sim \frac{C_j^*(\vec{k}_4)}{|\vec{k}_3 - \vec{k}_1|^2 + k_{TF}^2} , \tag{14}$$

where the subscript "0" is to be associated with $\vec{G} = 0$ and for weak pseudopotentials $C_0(\vec{k}_i) \simeq 1$. If the number of plane waves included in Eq. (6) is increased, the coefficient of the original $\vec{G} \neq 0$ plane waves tends to decrease. Thus the magnitude of the terms in Eq. (9) tends to decrease and while there will be more nonzero terms in the sum, they tend not to add coherently so that the typical matrix element is reduced. We believe that most of the remaining discrepancy is due to inaccuracy in their estimate of the phase space available for umklapp scattering. We make the comparison in terms of the quantity $\bar{\gamma}_\mu/\gamma$ [see their Eqs. (3.11)] which reflects the reduction in umklapp scattering due to phase-space restriction and the decrease in $V^{TF}(q) = 4\pi e^2/(q^2 + k_{TF}^2)$ with increasing q. (The typical q is larger for the umklapp events.) They have estimated that $\bar{\gamma}_\mu/\gamma \sim \frac{5}{9}$ for the alkali metals. Comparing their Eq. (3.11) with Eqs. (A3) we see that when $k_{TF}/k_F \to \infty$ (i.e., $r_s \to \infty$), $\bar{\gamma}_\mu/\gamma \to 2P_{G_{110}}$, where from Eq. (A5)

$$P_{G_{110}} = \sqrt{2}[(4\pi/3)^{-1/3} + \tfrac{1}{8}(4\pi/3)^{-1/3}] - 1 \simeq 0.1623 .$$

Moreover, from Fig. 1 we note that when r_s decreases from ∞ to the alkali-metal-density regime, $\bar{\gamma}/\gamma$ should decrease by a factor of ~3 to 4 due to the increasing q dependence of $V^{TF}(q)$ for $q \sim k_F$. Thus we expect that a better estimate of γ_μ/γ for the alkali-metal-density regime would be $\bar{\gamma}_\mu/\gamma \sim 0.1$.

The combined influence of the various improvements to the calculation of Lawrence and Wilkins[3] is to lead to a much smaller prediction for the Coulomb electron-electron scattering contribution to the resistivity of the alkali metals. Before giving detailed predictions, however, in the next section we repeat these calculations using accurate nonlocal model potentials and by carefully considering many-body effects on the quasiparticle velocities and wave functions.

III. NONLOCALITY AND MANY-BODY INFLUENCES ON Δ

We first consider many-body influences on the quasiparticle energies and wave functions. To avoid complicating the discussion we assume that the applied potential [the pseudopotentials $V_p(q)$ located on the lattice sites] is local. The quasiparticle energies and wave functions can be determined from the Green's function in the presence of the applied potential which obeys the Dyson equation[13,15]

$$G_{ij}(\vec{k}, \omega) = \delta_{i,j} G_j^0(\vec{k}, \omega) + \sum_{l,m} \delta_{i,l} G_l^0(\vec{k}, \omega)[\delta_{l,m} \Sigma_l(\vec{k}, \omega) + V_{\text{eff}}^l(\vec{G}_l - \vec{G}_n)] G_{mj}(\vec{k}, \omega) , \tag{15}$$

where $\vec{k}$ is in the first Brillouin zone (BZ), $G_j^0(\vec{k}, \omega)$ $[\Sigma_j(\vec{k}, \omega)]$ is the noninteracting uniform-system Green's function (uniform-system self-energy) evaluated at wave vector $\vec{k} + \vec{G}_j \equiv \vec{k}_j$, and

$$V_{\text{eff}}^l(q) = \tilde{\Lambda}(\vec{k}_l, q) V_p(q)/\epsilon(q) . \tag{16}$$

In Eq. (16), $\tilde{\Lambda}$ is the irreducible vertex function and $\epsilon(q)$ the dielectric function of the homogeneous system. We have anticipated our interest in solving for only the quasiparticle part of the full Green's function in ignoring the energy dependence of $\tilde{\Lambda}$.[16] The position-space representation of the Green's function is related to the double-wave-vector representation of Eq. (15) by

$$G(\vec{r}, \vec{r}'; \omega) = \frac{1}{\Omega} \sum_{\vec{k} \in BZ} \sum_{i,j} \exp(i\vec{k}_i \cdot \vec{r}) G_{ij}(\vec{k}, \omega) \times \exp(-i\vec{k}_j \cdot \vec{r}) . \tag{17}$$

In matrix notation Eq. (15) may be rewritten as

$$[\underline{G}(\vec{k}, \omega)]_{ij}^{-1} = [\omega - |\vec{k} + \vec{G}_i|^2 - \Sigma_i(\vec{k}, \omega)]\delta_{i,j} + V_{\text{eff}}^i(\vec{G}_i - \vec{G}_j) . \tag{18}$$

In keeping with the approximations of Sec. II, we wish to solve Eq. (18) for $|\vec{k}| = k_F$. Thus we may consider only terms to leading order in $\omega - \mu^0$

where μ^0 is the quasiparticle energy at $|\vec{k}| = k_F$ in the absence of the perturbation. For this case Eq. (18) may be rewritten as

$$[\underline{G}(\vec{k}, \omega)]^{-1}_{ij} \simeq Z^{-1}\{\omega - \mu^0 - Z[\Sigma_i(k_F, \mu^0) + k_i^2 - \Sigma_0(k_F, \mu^0) - k_F^2]\}\delta_{i,j} + Z V^i_{\text{eff}}(\vec{G}_i - \vec{G}_j) \quad (19)$$

(recall that $\vec{G}_0 \equiv 0$), where Z is the uniform-system quasiparticle renormalization factor. Thus the effective interaction determining the Fermi surface has a contribution from the $\vec{k}$ dependence of the homogeneous system self-energy in addition to the usual effective interaction used in calculating transport properties. In their consideration of the influence of a pseudopotential on quasiparticle energies and wave functions, Heine *et al.* have treated only the case in which G^{-1} can be truncated to wave vectors satisfying $k_i \simeq k_j \simeq k_F$. In this case the additional contribution vanishes. However, a general $\vec{k}$ point on the Fermi surface is not capable of satisfying $|\vec{k} + \vec{G}_j| = k_F$, so that their analysis has little bearing on the Fermi surface of a simple metal. Thus the identity of scattering potential determining the shape of the Fermi surface and the electron-ion interaction form factor frequently claimed in the literature[17] does not in general hold. Nevertheless, as is noted below, this identification may be an adequate approximation in many instances.

It follows from Eqs. (19) and (17) that for ω near μ^0 and k near k_F,

$$G_{ij}(\vec{k}, \omega) = \frac{Z C_i C_j^*}{\omega - E_k}, \quad (20)$$

where E_k is the eigenvalue of $(\omega - Z^{-1}G^{-1})$ [Eq. (19)] near μ^0 and $\{C_i\}$ is the associated eigenvector. Thus E_k is the quasiparticle energy and the quasiparticle wave function is related to $\{C_i\}$ as in Eq. (6). We have solved the eigenvalue equation by standard matrix techniques. Σ and Z were taken from the calculations of MacDonald *et al.*[18] The RT pseudopotentials (see Table II), including their nonlocality, were used. For $\tilde{\Lambda}$, whose dependence on $\vec{k}_i$ is not well known, we have substituted the Fermi surface to Fermi-surface values suggested by Rasolt.[19] With this approximation the potential in Eq. (19) is identical to the potential appearing in transport theory. We note that for $|k_i - k_F| \ll k_F$ the diagonal self-energy term in Eq. (19) satisfies

$$Z[\Sigma_i(k_F, \mu^0) + k_i^2 - \Sigma_0(k_F, \mu^0) - k_F^2] \simeq (k_i^2 - k_F^2)/m^* . \quad (21)$$

(We have not adopted this approximation here.) If both the approximation for $\tilde{\Lambda}$ and Eq. (21) are adopted, the resulting quasiparticle energies and wave functions will be identical, aside from an effective-mass correction to the unperturbed energies, to those calculated using the transport theory form factors. Thus the identification of these two effective potentials while not exact is a reasonable approximation.

The values of Δ obtained from Eq. (19) are listed in Table III. We note that the values of Δ_0 show a tendency to increase with nonlocality. This can be understood partly in terms of the expression for the quasiparticle velocity corresponding to Eq. (19):

$$V_{\vec{k}} = Z\sum_{i,j} C_i^*\left[\left(2\vec{k}_i + \frac{\partial\Sigma}{\partial\vec{k}}(k_i, \mu^0)\right)\delta_{i,j} + \nabla_{\vec{k}} V^i_{\text{eff}}(\vec{G}_i - \vec{G}_j)\right]C_j . \quad (22)$$

Δ_0 is a measure of the anisotropy of $|V_{\vec{k}}|$ over the Fermi surface. For a local effective potential $\nabla_{\vec{k}} V^i_{\text{eff}}(\vec{G}_i - \vec{G}_j) = 0$, but as indicated in Fig. 3, the effective potential is highly nonlocal for all the alkali metals except Na. This extra contribution to $V_{\vec{k}}$ adds to the anisotropy of $|V_{\vec{k}}|$ and increases Δ_0. The changes in Δ_1 on including nonlocality depend on the metal. The approximation of Sec. II amounts to replacing in $V^i_{\text{eff}}(\vec{G}_i - \vec{G}_j)$ by its value when $\hat{k}_i \cdot \hat{k}_j = -1$. From Fig. 3 we see that, except for the case of Na, this replacement entirely misrepresents the matrix elements of the effective potential. For Li, Δ_1 is increased even though the mean value of V_{110} is reduced. This

TABLE III. Results for the fractional umklapp scattering Δ in the alkali metals with nonlocality effects included (see text). These results were obtained using the RT pseudopotentials (see Table II).

Metal	Δ_0	Δ_1	Δ_2	Δ_3	Δ(%)
Li	2.4×10^{-3}	1.3×10^{-3}	4×10^{-6}	1×10^{-9}	0.37
Na	1×10^{-5}	5×10^{-4}	2×10^{-5}	3×10^{-10}	0.05
K	7×10^{-6}	7×10^{-4}	2×10^{-6}	6×10^{-11}	0.07
Rb	1.3×10^{-3}	7×10^{-4}	1×10^{-6}	6×10^{-11}	0.20
Cs	7.7×10^{-3}	8×10^{-4}	3×10^{-6}	6×10^{-10}	0.85

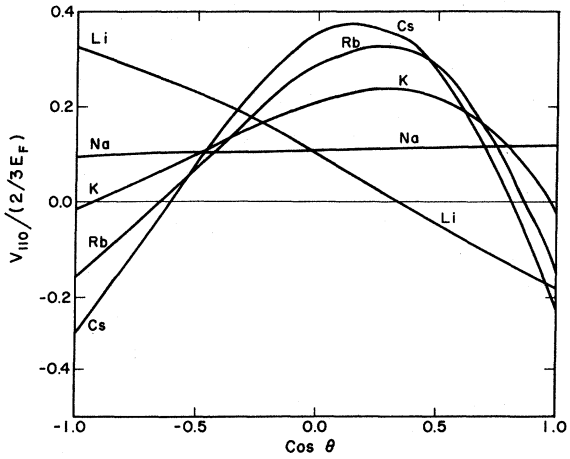

FIG. 3. Screened pseudopotential form factors $\langle \vec{k}+\vec{G}| W|\vec{k}\rangle$ for the alkali metals as a function of $\cos\theta \equiv (\vec{k}+\vec{G})\cdot(\vec{k})/|\vec{k}+\vec{G}|$. For a local pseudopotential the form factors are independent of $\cos\theta$. The backscattering matrix element corresponds to $\cos\theta = -1$ so that approximation of Sec. II amounts to replacing each of these curves by a horizontal line with the same position at the left axis.

is because for some $\hat{k}_i \cdot \hat{k}_j$, V_{110} enters the larger Δ_1/V_{110}^2 region of negative V_{110} values (see Fig. 2). For K the backscattering value of V_{110} is anomalously small and its use in Sec. II has strongly underestimated the strength of the electron-ion interaction. For Rb and Cs much of the decrease in Δ_1 when nonlocality is included can be attributed to V_{110} being positive for most values of $\hat{k}_i \cdot \hat{k}_j$ (see Fig. 2). In addition it appears that the change in sign of V_{110} as a function of $\hat{k}_i \cdot \hat{k}_j$ causes some cancellation to occur in the evaluation of matrix elements via Eq. (9). The total values for Δ listed in Table III range from less than 0.1% in the most jelliumlike of the alkali metals Na and K, to nearly 1% in the metal with the largest crystalline effects, Cs. In the next section these values for Δ are combined with estimates of τ_0^{-1} to obtain the A_{ee} which would be expected on the basis of Coulomb scattering only.

IV. ELECTRON-ELECTRON SCATTERING RESISTIVITY FOR COULOMB SCATTERING ONLY

The electron-electron scattering coefficients obtained by combining the values of Δ listed in Table III with the approximations of Ref. 14 for the Coulomb-only electron-electron scattering rate, τ_0^{-1}, are listed in Table IV ($\tau_0^{-1} \propto A_{ee}/\Delta$). The accuracy of the method of Ref. 14 for calculating τ_0^{-1} has been firmly established by comparison of theoretical and experimental values for the Lorenz function of the alkali metals above Θ_D.[20] For the purpose of comparison we have also listed in Table IV the values obtained for A_{ee}/Δ when the Born-Thomas-Fermi approximation for the scattering amplitudes [Eq. (4)] is adopted (A_{ee}^{TF}/Δ). When an effective-mass correction is applied[21] (parenthetical numbers in Table IV), the values predicted by this approximation are surprisingly accurate, being a factor of ~2 too small. This accuracy is due in part to a cancellation of errors since the Born approximation will overestimate the scattering amplitude for a given effective interaction[22] while the Thomas-Fermi approximation underestimates the effective interaction.[23] Nevertheless, this accuracy does lend some credence to the claim that Δ, being the ratio of two different integrals in which the transition probability plays the role of a weighting factor, can be estimated using the Born-Thomas-Fermi approximation.

To date, experimental work on the low-temper-

TABLE IV. Electron-electron scattering resistivity calculated including only the Coulomb interaction. A_{ee}/Δ was calculated using the accurate Fermi-liquid theory of Ref. 14 for the scattering amplitude. For comparison we have also listed the value obtained for this quantity when the Thomas-Fermi approximation is used for the scattering amplitude A_{ee}^{TF}/Δ. The theoretical value listed for A_{ee} is $(A_{ee}/\Delta)\Delta$. The values in parentheses under A_{ee}^{TF}/Δ include an effective-mass correction as discussed in the text.

Metal	A_{ee}/Δ 10^{-15} ΩmK^{-2}	A_{ee}^{TF}/Δ 10^{-15} ΩmK^{-2}	Δ %	$A_{ee}(10^{-17}$ ΩmK$^{-2})$ Theory	Expt.
Li	15	3(8)	0.37	6	~2000 [a]
Na	19	9(11)	0.05	1	180–195 [b]
K	59	31(38)	0.07	4	55–290 [c]
Rb	79	39(46)	0.20	16	
Cs	150	56(85)	0.85	130	

[a] Reference 9.
[b] Reference 11.
[c] References 10 and 11.

ature resistivity of the alkali metals has been undertaken for Li (Ref. 9), K (Refs. 10 and 11), and Na (Ref. 11). For K the interpretation of the results is confused by the apparent sample dependence of A_{ee}. The earlier work on Li is probably less reliable than the very accurate recent work on Na and K. We do not discuss the results at this point beyond noting that for both Na and K the experimental values of A_{ee} are 1 to 2 orders of magnitude larger than those which we have obtained theoretically. We believe that, as discussed in the next section, this discrepancy is principally due to the failure to include the phonon-exchange contribution to the scattering amplitude. However, we should first mention two additional sources of uncertainty in the above theoretical predictions.

As noted in Eq. (12) the values of Δ listed in Table III reflect primarily the fraction of the weight of states $|\vec{k}\rangle$ on the Fermi surface associated with plane waves $\exp[i(\vec{k}+\vec{G}_j)\cdot\vec{r}]$ for $\vec{G}_j \neq 0$. We have implicitly assumed that these higher plane-wave coefficients are not strongly influenced by the core-orthogonalization component of the wave function, which is absent in the pseudowave function. The importance of the core-orthogonalization components should be larger in the larger core systems. MacDonald[24] has compared the coefficient of the $\exp[i(\vec{k}-\vec{G})\cdot\vec{r}]$ plane wave obtained by expanding the true solid-state wave function with the corresponding coefficient of the pseudowave function for a point on the Fermi surface near the $\vec{k}\cdot\vec{G}=G^2/2$ Bragg plane for several alkali metals. The ratio of these coefficients was found to be 1.3, 1.6, and 1.7 for Li, Rb, and Cs indicating that our estimates of Δ could be increased by at most a factor of ~3 as a result of including core-orthogonalization components of the wave function. This would not be sufficient to resolve the discrepancy indicated in Table IV.

A second deficiency of the calculation leading to the values of Δ listed in Table III is that we have used an effective electron-electron interaction which depends only on the distance between electrons. In a real solid the scattering function will not be fully translationally invariant so that, even in a 1-plane-wave approximation for the pseudowave function there will be nonzero contribution to Δ. The potential size of this contribution to Δ for Na can be estimated from the examination of Hedin *et al.*[25] of the off-diagonal terms in a representation for the dielectric function similar to that used for the Green's function in Sec. III (see the discussion in Ref. 26). For Na this contribution to Δ will be at most ~0.1%. It is clear that this contribution to Δ will be, at most, about the same order as the contribution which we have calculated.

V. ELECTRON-ELECTRON SCATTERING RESISTIVITY INCLUDING PHONON-EXCHANGE SCATTERING

In metals, electrons interact both via Coulomb repulsion and via the attraction caused by the virtual exchange of phonons. We have thus far ignored the latter interaction. In superconducting simple metals the phonon-mediated interaction is expected to be stronger, but for the alkali metals the importance of this interaction is less obvious. In Table V we have listed values of A_{ee}/Δ for the alkali metals obtained using the approximations of Ref. 14 with Coulomb interactions only, phonon-exchange interactions only, and both interactions.[27] As noted in Ref. 27 the strength of the attractive phonon-exchange interaction relative to that of the replusive Coulomb interaction may be crudely characterized by a parameter, C_{ep} (see Ref. 27). The values of this parameter for the alkali metals

TABLE V. A_{ee}/Δ from Coulomb interactions only (A_{ee}^{C}/Δ) from phonon-exchange interactions only (A_{ee}^{PX}/Δ) and including both interactions (A_{ee}^{CPX}/Δ). A_{ee}/Δ is a measure of the rate at which quasiparticles are scattered by normal electron-electron events. All quantities are given in units of $10^{-15}\ \Omega m K^{-2}$. All these quantities were calculated using the approximations of Ref. 14. C_{ep} is a measure of the ratio of the strengths of the two interactions as discussed in the text. Also listed is the value of A_{ee}^{PX}/Δ obtained in an "exact" calculation as discussed in the text and the parameter X which characterizes the A_{ee}^{CPX}/Δ obtained when the Thomas-Fermi approximation to the Coulomb interaction is combined with the exact expression for the phonon-exchange interaction (see text).

Metal	A_{ee}^{C}/Δ	A_{ee}^{PX}/Δ (exact)	C_{ep}	A_{ee}^{PX}/Δ (Ref. 14)	X [see Eq. (28)]	A_{ee}^{CPX}/Δ
Li	15	8	0.59	8	−0.01	5
Na	19	10	0.70	7	0.14	5
K	59	12	0.48	8	−0.05	30
Rb	79	15	0.42	10	0.05	43
Cs	150	23	0.34	14	0.08	96

are listed in Table V. It is immediately apparent from these values that, at least for the lighter elements in the alkali series, the phonon-exchange process cannot be ignored. When both interactions are included using the methods of Ref. 14, there is a cancellation between repulsive and attractive interactions and the scattering rate is reduced below that obtained in the Coulomb-only case. (It should be emphasized that $A_{ee}/\Delta \propto \tau_0^{-1}$ measures the total scattering rate which is dominated by normal scattering events.) We have discussed in Secs. II and III the considerations determining the Coulomb-only umklapp scattering rate. In order to discuss the umklapp scattering rate in the presence of both interactions we follow Rice[28] in observing that in the zero-energy-transfer limit only the diagrams of Fig. 4 contribute to the phonon-exchange scattering function. Thus for the phonon-exchange-only case it follows that

$$\omega_{\uparrow\uparrow}(\vec{k}_1,\vec{k}_2;\vec{k}_1'\vec{k}_2') \simeq \frac{2\pi}{\hbar}\left|g_\lambda(\vec{k}_1',\vec{k}_1)g_\lambda(\vec{k}_2',\vec{k}_2)\mathfrak{D}_\lambda(\vec{k}_1'-\vec{k}_1) - g_\lambda(\vec{k}_2',\vec{k}_1)g_\lambda(\vec{k}_1',\vec{k}_2)\mathfrak{D}_\lambda(\vec{k}_2'-\vec{k}_1)\right|^2 , \tag{23}$$

where summation over the repeated phonon polarization index is implied:

$$g_\lambda(\vec{k}',\vec{k}) \simeq -(\Omega_0/2MZ^2\Omega_{\vec{q},\lambda})^{1/2} \times \hat{e}_{\vec{q},\lambda}\cdot\sum_{i,j} C_i^*(\vec{k}')C_j(\vec{k})(\vec{k}_i'-\vec{k}_j)\frac{V_{\text{eff}}^I(\vec{k}_i'-\vec{k}_j)}{m^*} . \tag{24}$$

$\Omega_{\vec{q},\lambda}$ and $\hat{e}_{\vec{q},\lambda}$ are the phonon frequencies and polarizations, Z is the valence, Ω_0 is the unit-cell volume, and in the zero-transfer limit the renormalized phonon propagator

$$\mathfrak{D}_\lambda(\vec{k},\vec{k}) \simeq \frac{-2}{\Omega_{\vec{q},\lambda}} . \tag{25}$$

The effective-mass correction factor m^{*-1} in Eq. (24) is discussed below. In these equations $\vec{q}$ is understood to represent $\vec{k}'-\vec{k}$ reduced to the first Brillouin zone. The effective electron-ion interaction appearing in Eq. (23) should include quasiparticle renormalization and screening corrections to the bare interaction.[28,29] [The opposite-spin scattering probability would be like Eq. (23) except that the exchange term would not appear.]

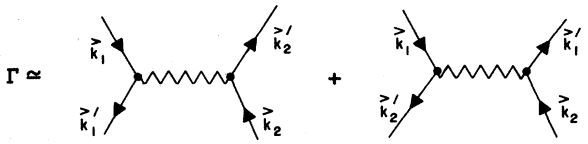

FIG. 4. The phonon-exchange contribution to the four-point scattering function in the zero-energy-transfer ($q/\omega \to \infty$) limit. The dots represent electron-phonon interaction vertices and the wavy line a renormalized phonon propagator.

We have calculated the electron-electron scattering rate obtained when Eq. (23) is used for the transition probability and these exact results are compared with the Ref. 14 approximation results in Table V. The phonons were calculated using the model potential method of Dagens, Rasolt, and Taylor.[30,31] The electron-ion interaction vertex was approximated by using a single-plane-wave approximation for the pseudowave function in Eq. (24). The accuracy of this approximation in the alkali metals has been established in calculating the phonon-limited electrical resistivity.[32-34] We note that the Ref. 14 approximation results agree quite well with the "exact" results. This gives us added confidence in the analysis presented elsewhere for Al.[27] The situation becomes less satisfactory, however, when the Coulomb and phonon-exchange scattering mechanisms are included together. The difficulty is that no simple accurate expression analogous to Eq. (23) exists in the general case. Nevertheless, from the many-body-theory expressions for the full scattering function[35,27] it is clear that we may regard the effective interaction crudely as the sum of Coulomb and phonon-exchange interactions. Thus we choose to approximate

$$\omega_{\uparrow\uparrow}(\vec{k}_1,\vec{k}_2;\vec{k}_1',\vec{k}_2') \simeq \frac{2\pi}{\hbar}\left[\left(\frac{\alpha}{m^*}\langle\vec{k}_1',\vec{k}_2'|V^{\text{TF}}|\vec{k}_1,\vec{k}_2\rangle + \frac{g_\lambda(\vec{k}_1',\vec{k}_1)g_\lambda(\vec{k}_2',\vec{k}_2)}{m^{*2}}\mathfrak{D}_\lambda(\vec{k}_1'-\vec{k}_1)\right) - \left(\frac{\alpha}{m^*}\langle\vec{k}_2',\vec{k}_1'|V^{\text{TF}}|\vec{k}_1,\vec{k}_2\rangle + \frac{g_\lambda(\vec{k}_2',\vec{k}_1)g_\lambda(\vec{k}_1',\vec{k}_2)}{m^{*2}}\mathfrak{D}_\lambda(\vec{k}_2'-\vec{k}_1)\right)\right]^2 , \tag{26}$$

with the exchange term being absent for the opposite-spin scattering case. The m^* factors in Eq. (26) approximately account for the influence of the Fermi-level density of states on the screening functions.[14,27] Ignoring electron-electron interaction mass renormalizations, we took

$$m^* = m_b(1+\lambda) \tag{27}$$

with m_b and λ chosen as in Ref. 14 and all masses in free-electron mass units. The factor α in Eq. (26) is to be chosen so as to compensate for our ignorance of the Coulomb contribution to the scat-

TABLE VI. Contributions to the electron-electron scattering resistivity from scattering events associated with the first four shells of reciprocal-lattice vectors. The results reported here are for $\alpha=\alpha^*$ (see text). The values of Δ are in %.

Metal	A_{ee}/Δ (10^{-15} ΩmK^{-2})	Δ_0	Δ_1	Δ_2	Δ_3	Δ	A_{ee} (10^{-17} ΩmK^{-2})
Li	40	0.17	3.11	0.57	1.52	5.38	210
Na	40	0.00	3.48	0.02	0.00	3.50	140
K	80	0.00	2.05	0.01	0.00	2.07	170
Rb	130	0.13	2.24	0.23	0.17	2.77	350
Cs	240	0.73	1.25	0.23	0.62	2.82	670

tering function. The scattering rate obtained with Eq. (26) is expressed in Table V in terms of the quantity X which is related to the electron-electron scattering rate by

$$v_{ee}(\alpha)=v_{ee}^{PX}+2X\alpha m^*\sqrt{v_{ee}^{PX}v_{ee}^{TF}}+\alpha^2 m^{*2}v_{ee}^{TF}\ , \tag{28}$$

where

$$A_{ee}/\Delta=(m^*r_s^3/34.1)(v_{ee}/T^2)10^{-21} \tag{29}$$

in units of Ωms. Crudely speaking, $X=1$ would correspond to the two interactions adding together in a coherent fashion while $X=-1$ would correspond to the interactions canceling against each other to the greatest possible degree. It is clear that the approximations of Ref. 14 predict a much greater degree of cancellation than does Eq. (26). The reason is that in the Thomas-Fermi approximation the parallel-spin scattering amplitude is very small since direct and exchange terms nearly cancel.[36] The phonon-exchange direct and exchange terms cancel to a much lesser degree so that amplitudes for parallel-spin scattering increase. On the other hand, amplitudes for opposite-spin scattering decrease in the expected manner leading to the near zero values of X.

Since the many-body-theory approach of Ref. 14 properly includes the rather subtle way in which phonon-exchange and Coulomb interactions combine to form a net interaction, we tend to favor the scattering rates predicted by that approach. However, this approach cannot predict the scattering amplitudes for umklapp events, so we must use Eq. (26) in order to calculate A_{ee}. Fortunately almost all the amplitude for umklapp scattering events comes from the phonon-exchange process so that the predicted values of A_{ee} will be insensitive to α. The values obtained for A_{ee} are listed in Table VI and are increased over those obtained with Coulomb scattering only by factors varying

TABLE VII. Values of A_{ee} obtained for the alkali metals including both Coulomb and phonon-exchange scattering mechanisms. The dependence of A_{ee} on the scaling correction to the Thomas-Fermi Coloumb interaction is indicated. For comparison we have listed the value of A_{ee} obtained when phonon-exchange scattering is neglected, A_{ee}^{CO}. The coefficient of T^5 in the low-temperature phonon-limited resistivity A_{ep} and the temperature at which $A_{ep}T^5=A_{ee}(\alpha^*)T^2(T_e)$ are also listed. A_{ee} is in units of 10^{-17} ΩmK^{-2} and A_{ep} in units of 10^{-17} ΩmK^{-2}.

	Li	Na	K	Rb	Cs
A_{ee}^{CO}	6	1	4	16	130
α^*	1.39	1.31	1.25	1.31	1.33
A_{ee} ($\alpha=0$)	200	130	170	330	500
A_{ee} ($\alpha=1$)	210	130	170	340	570
A_{ee} ($\alpha=\alpha^*$)	210	140	170	350	670
A_{ee} (expt)	~2000 [a]	180–195 [b]	55–290 [c]		
A_{ep}	0.02 [d]	5 [d]	25 [e]	270 [f]	1400 [f]
T_e (K)	22	3	1.9	1.1	0.8

[a] Reference 9.
[b] Reference 11.
[c] References 10 and 11.
[d] Reference 32.
[e] Reference 33.
[f] Reference 34.

from ~5 in Cs to ~150 in Na. The calculations were performed with $\alpha = \alpha^*$ where α^* is the value of α which brings A_{ee}^{TF}/Δ and A_{ee}^{FL}/Δ (FL for Fermi liquid) into agreement *without* the phonon-exchange scattering being present. In Table VII the weak dependence of A_{ee} on α is explicitly exhibited and the magnitude of A_{ee} is compared with the coefficient of T^5 in the low-temperature phonon-limited resistivity to predict the temperature, T_e, at which the two contributions to ρ should be equal.[37] Presumably convincing identifications of T^2 components in the resistivity would require the ideal resistivity to be accurately measured at least down to temperatures $\sim T_e/2$.

The interpretation of existing experiments on the low-temperature ρ of K is somewhat confused and so the comparison with experiment in Table VII deserves a few words of elaboration. The experimental value of A_{ee} obtained by fitting $\rho(T)$ to an assumed T^2 dependence has been observed to be sample dependent. This sample dependence has been interpreted by Kaveh and Wiser[38,11] as being due to interference between electron-electron and anisotropic electron-defect scattering. If their interpretation is correct, the ideal T^2 coefficient should correspond to the lowest values of A_{ee} obtained experimentally. However, Rowlands *et al.* have found that the $\rho(T)$ for T in the range ~0.5 to 1.5 K, used in the analysis of Kaveh and Wiser, varies more nearly like $T^{1.5}$ rather than like T^2. Recently Schroeder *et al.* have found that below $T = 0.5$ K a T^2 fit is again better and they find $A_{ee} \simeq 230 \times 10^{-17} \Omega m\ \mathrm{K}^{-2}$. It is not yet known if the coefficient of T^2 in this extreme low-temperature region is sample dependent. The experimental value obtained for Li (Ref. 9) does not seem to be consistent with the more recent work on Na and K. The case of Li ought to be re-examined. It is possible, but we believe unlikely, that band-structure effects need to be explicitly accounted for in Li.

VI. CONCLUDING REMARKS

We have calculated the electron-electron scattering coefficient in the low-temperature electrical resistivity for the alkali metals, including both Coulomb and phonon-exchange scattering processes. It has been demonstrated that the value for A_{ee} obtained including only the Coulomb scattering process has been seriously overestimated in an earlier calculation and that, in fact, the value of A_{ee} is dominated by the phonon-exchange scattering process. The values obtained for A_{ee} are consistent with existing experiments on the low-temperature $\rho(T)$ of Na and K. However, apparent sample dependence of the experimental results and apparent slower-than-T^2 increases in $\rho(T)$ for $T \sim 0.5$ to 1.5 in K, have confused the interpretation of these experiments. Size effects[10,39] and electron-phason scattering associated with a possible charge-density-wave ground state[40] have been suggested as other possible explanations of the observed behavior. Further experimental and theoretical effort should allow a clear conclusion to emerge. It is our expectation that the results obtained here, which we believe to be quantitatively accurate for the ideal system with a normal ground state, will play a useful role in this process.

APPENDIX

It is sufficient to consider integrals of the form

$$\langle F_i \rangle = \left(\frac{2}{k_F}\right)^4 \int \prod_{i=1}^{4} [d\vec{k}_i \delta(k_i^2 - k_F^2)] \times \delta(\vec{k}_1 + \vec{k}_2 - \vec{k}_3 - \vec{k}_4 + \vec{G}_i)\omega F \,, \tag{A1}$$

where the arguments of ω and F have been dropped. The integral over one wave vector and the radial portion of the remaining wave-vector integrals may be performed trivally to yield

$$\langle F_i \rangle = \int d\vec{e}_1 \int d\vec{e}_2 \int d\vec{e}_3 \delta\left(\frac{K}{2} - \vec{K}\cdot\vec{e}_3\right)\omega F \,, \tag{A2}$$

where $\vec{k}_i = k_F \vec{e}_i$, $\vec{k}_4 = \vec{k}_1 + \vec{k}_2 + \vec{G}_i - \vec{k}_3$, and $\vec{K} = (\vec{k}_1 + \vec{k}_2 + \vec{G})/k_F$. In performing the integral over $\vec{e}_3$ we let $\vec{K}$ be the polar axis. (Denote the polar coordinates by $\cos\theta_3 = u_3$ and ϕ_3.) Note that the argument of the δ function can be zero only if $K < 2$. This condition restricts the available phase space for the $\vec{e}_1$ and $\vec{e}_2$ integrals. It is essential for this restriction of the range of integration to be accounted for explicitly if F_i is to be accurately evaluated. To do this conveniently it is necessary to let $\vec{k}_1 + \vec{G}_i$ be the polar axis in performing the integral over $\vec{e}_2$ and to let $\vec{G}_i$ be the polar axis for integrating over e_1, the polar coordinates being denoted by $(\cos\theta_2 = \mu_2, \phi_2)$ and $(\cos\theta_1 = \mu_1, \phi_1)$, respectively. When this is done we obtain

$$\langle F_i \rangle = 0, \quad G \geq 4k_F = \int_0^{2\pi} d\phi_1 \int_0^{2\pi} d\phi_2 \int_0^{2\pi} d\phi_3 \int_{-1}^{\mu_1^{MAX}} \int_{-1}^{\mu_2^{MAX}} \frac{\omega F}{K}, \quad G \leq 4k_F \,, \tag{A3a}$$

where

$$\mu_1^{\mathrm{MAX}} = \begin{cases} 1, & G \leq 2k_F \\ \dfrac{8-(G/k_F)^2}{2(G/k_F)}, & G \geq 2k_F \end{cases} \tag{A3b}$$

and

$$\mu_2^{\mathrm{MAX}} = \begin{cases} \left[1-1/2\left(\dfrac{G}{k_F}\right)^2-\left(\dfrac{G}{k_F}\right)\mu_1\right]\Big/\left[1+\left(\dfrac{G}{k_F}\right)^2+2\left(\dfrac{G}{k_F}\right)\mu_1\right]^{1/2}, & \left[1+\left(\dfrac{G}{k_F}\right)^2+2\left(\dfrac{G}{k_F}\right)\mu_1\right] > 1 \\ 1 \text{ otherwise} . \end{cases} \tag{A3c}$$

The coordinates of $\vec{k}_1, \vec{k}_2, \vec{k}_3$, and $\vec{k}_4$ in the crystal coordinate system can be obtained from the five polar coordinates in Eq. (A3a) by using rotation matrices. For the $\vec{G}=0$ case the polar axis for the $\vec{e}_1$ integral may be chosen arbitrarily.

The five-dimensional integral in Eq. (A3a) can be evaluated numerically using product Gauss quadrature. Special care should, however, be taken whenever

$$K = \{2+(G/k_F)^2+2(G/k_F)\mu_1 + 2[1+(G/k_F)^2+2(G/k_F)\mu_1]^{1/2}\mu_2\}^{1/2} \tag{A4}$$

becomes zero inside the range of integration. For the case of interest here, monovalent bcc metals, this can only happen for $G=0$. In that case, an integration formula of the Gaussian type in which the $(1+\mu_2)^{-1/2}$ factor is explicitly accounted for can be used for the $d\mu_2$ integration. It should be noted that for all cases of interest here, F_i has the same value for all reciprocal-lattice vectors in a given shell.

Equations (A3) may be used to compare the phase space available for normal scattering events to that available for umklapp scattering events. For a given reciprocal-lattice vector of magnitude G the ratio of the phase space available for the associated umklapp events to the phase space available for normal events is

$$P_G = \begin{cases} 1-\dfrac{3(G/k_F)}{8}, & \left(\dfrac{G}{k_F}\right) \leq 2 \\ \dfrac{(4k_F-G)^2}{8Gk_F}, & 2 \leq \left(\dfrac{G}{k_F}\right) \leq 4 \\ 0, & \left(\dfrac{G}{k_F}\right) \geq 4 . \end{cases} \tag{A5}$$

The phase space available for normal and umklapp scattering events is compared for bcc, fcc, and (ideal) hcp crystal structures in Table VIII. Note that the total umklapp phase space is not sensitive to crystal structure.

TABLE VIII. Phase space available for normal and umklapp scattering events in bcc, fcc, and (ideal) hcp metals. The reciprocal-lattice vector $\vec{G}$ associated with an event is indicated by (hkl) where $\vec{G}=(2\pi/a)(h,k,l)$ for bcc and fcc and $\vec{G}=(2\pi/a)(h,k/\sqrt{3},(a/c)l)$ for hcp. N_G is the number of members of a shell and Z is the valence.

			$P_G N_G$			
Structure	$\vec{G}$	N_G	$Z=1$	$Z=2$	$Z=3$	$Z=4$
bcc	(000)	1	1.000	1.000	1.000	1.000
bcc	(110)	12	1.947	3.858	4.887	5.537
bcc	(200)	6	0.140	0.609	1.045	1.432
bcc	(211)	24	0.002	0.718	1.746	2.759
bcc	(220)	12	0.000	0.040	0.225	0.443
bcc	(310)	24	0.000	0.000	0.184	0.581
bcc	(222)	8	0.000	0.000	0.004	0.066
bcc	(321)	48	0.000	0.000	0.000	0.064
	$\sum P_G N_G$		3.089	6.225	9.091	11.882
fcc	(000)	1	1.000	1.000	1.000	1.000
fcc	(111)	8	1.436	2.723	3.390	3.812
fcc	(200)	6	0.609	1.432	2.008	2.373
fcc	(220)	12	0.040	0.443	1.329	1.947
fcc	(311)	24	0.000	0.356	1.141	1.976
fcc	(222)	8	0.000	0.066	0.280	0.523
fcc	(400)	6	0.000	0.000	0.043	0.140
fcc	(331)	24	0.000	0.000	0.014	0.202
fcc	(420)	24	0.000	0.000	0.001	0.130
fcc	(422)	24	0.000	0.000	0.000	0.002
	$\sum P_G N_G$		3.085	6.020	9.206	12.105
hcp	(000)	1	1.000	1.000		
hcp	(001)	2	0.953	1.169		
hcp	(110)	6	0.533	1.310		
hcp	(002)	2	0.131	0.359		
hcp	(111)	12	0.524	1.695		
hcp	(112)	12	0.010	0.448		
hcp	(003)	2	0.000	0.034		
hcp	(130)	6	0.000	0.030		
hcp	(131)	12	0.000	0.018		
hcp	(113)	12	0.000	0.002		
	$\sum P_G N_G$		3.151	6.065		

[1]L. Landau and I. Pomeranchuk, Phys. Z. Sowjetunion 10, 649 (1936).
[2]For example, M. J. Rice, Phys. Rev. Lett. 20, 1439 (1968).
[3]W. E. Lawrence and J. W. Wilkins, Phys. Rev. B 7, 2317 (1973).
[4]W. E. Lawrence, Phys. Rev. B 13, 5316 (1976).
[5]H. van Kempen, J. H. J. M. Ribot, and P. Wyder, J. Phys. C 6, 1048 (1978).
[6]J. H. J. M. Ribot, J. Bass, H. van Kempen, and P. Wyder, J. Phys. F 9, L117 (1979), and unpublished.
[7]M. Khoshnevisan, W. P. Pratt, P. A. Schroeder, and S. D. Steenwyk, Phys. Rev. B 19, 3873 (1979).
[8]M. Khoshnevisan, W. P. Pratt, P. A. Schroeder, S. Steenwyk, and C. Uher, J. Phys. F 9, L1 (1979).
[9]G. Krill, Solid State Commun. 9, 1065 (1971).
[10]H. van Kempen, J. S. Lass, J. H. J. M. Ribot, and P. Wyder, Phys. Rev. Lett. 37, 1574 (1976). See also J. A. Rowlands, C. Duvvury, and S. B. Woods, Phys. Rev. Lett. 40, 1201 (1978), and P. A. Schroeder, C. W. Lee, W. P. Pratt, and J. A. Rowlands, Bull. Am. Phys. Soc. 25, 211 (1980).
[11]B. Levy, M. Sinvani, and A. J. Greenfield, Phys. Rev. Lett. 43, 1822 (1979).
[12]For example, J. M. Ziman, *Electrons and Phonons* (Oxford University, London, 1963).
[13]V. Heine, P. Nozières, and J. W. Wilkins, Philos. Mag. 13, 741 (1966).
[14]A. H. MacDonald and D. J. W. Geldart, J. Phys. F 10, 677 (1980).
[15]L. Hedin and S. Lundqvist, Solid State Phys. 23, 1 (1969).
[16]It is understood that the pseudopotentials are to be treated to first order in perturbation theory. We ultimately require the vertex part to be evaluated at the new quasiparticle energy rather that at the unperturbed quasiparticle energy as in Eq. (16). The change in the vertex function with such a change in its energy argument would alter the quasiparticle energy and wave function only in higher order.
[17]For example, P. B. Allen and M. J. G. Lee, Phys. Rev. B 10, 3848 (1972).
[18]A. H. MacDonald, M. W. C. Dharma-wardana, and D. J. W. Geldart, J. Phys. F 10, 1719 (1980).
[19]M. Rasolt, J. Phys. F 5, 2294 (1975).
[20]In the alkali metals the derivation of the Lorenz function above Θ_D from its elastic scattering value is due to the electron-electron scattering contribution to the thermal resistivity W_{ee}. Since W_{ee} is only weakly influenced by the small amount of umklapp scattering present, the theoretical value for this quantity is nearly proportional to τ_0^{-1}.
[21]As emphasized in Ref. 14, A_{ee} is approximately proportional to the square of the Fermi-level density of states $g(\mu)$. We have incorporated this band-mass effect in the calculation of A_{ee}^{TF}/Δ using the values of the band mass discussed in Ref. 14.
[22]C. A. Kukkonen and H. Smith, Phys. Rev. B 8, 4601 (1973).
[23]C. A. Kukkonen and John W. Wilkins, Phys. Rev. B 19, 6075 (1979).
[24]A. H. MacDonald, J. Phys. F 10, 1737 (1980).
[25]L. Hedin, A. Johansson, B. I. Lundqvist, S. Lundqvist, and V. Samathiyakanit, Ark. Fys. 39, 97 (1969).
[26]L. Hedin and S. Lundqvist, Solid State Phys. 23, 1 (1969).
[27]Reference 14 deals explicitly with Coulomb interactions only. An application of this method to Al, which includes the electron-phonon contribution is described by A. H. MacDonald, Phys. Rev. Lett. 44, 489 (1980).
[28]T. M. Rice, Phys. Rev. 175, 858 (1968).
[29]All three correction factors are altered by the electron-phonon interaction and so this is not exactly the same effective interaction as the one which usually appears in transport theory. In metals with strong electron-phonon interactions it would be important to include these corrections, at least approximately.
[30]L. Dagens, Mark Rasolt, and Roger Taylor, Phys. Rev. B 11, 2726 (1975).
[31]Mark Rasolt and Roger Taylor, Phys. Rev. B 11, 2717 (1975); S. S. Cohen, M. L. Klein, M. S. Duesbery, and Roger Taylor, J. Phys. F 6, L271 (1976). Comparison of calculated and experimental phonon dispersions for Na are contained in this reference while those for Li and K are in Ref. 30. The corresponding comparison for Rb is contained in Ref. 34. The agreement obtained is generally better than that possible with a Born–von Karman fit.
[32]Roger Taylor and A. H. MacDonald, J. Phys. F 10, L181 (1980).
[33]Roger Taylor, C. R. Leavens, and R. C. Shukla, Solid State Commun. 19, 809 (1976).
[34]Roger Taylor and A. H. MacDonald, J. Phys. F 10, 2387 (1980).
[35]W. F. Brinkman, P. M. Platzman, and T. M. Rice, Phys. Rev. 174, 495 (1968).
[36]As the range of the interaction becomes smaller than the Fermi wavelength, parallel spins are unlikely to approach close enough to interact significantly. From Ref. 14 it is clear that the Thomas-Fermi approximation does not accurately describe the cancellation between direct and exchange terms.
[37]For Li, Rb, and Cs the onset of umklapp scattering at $T \sim \Theta_D/100$ causes the phonon-limited resistivity to rise much more sharply than the T^5 Bloch-Gruneisen behavior. Comparison of A_{ee} with the full calculated values of the phonon-limited resistivity would reduce the estimates of T_e to approximately 10, 0.8, and 0.6 K for Li, Rb, and Cs, respectively. The estimate of T_e would not be significantly altered for Na or K.
[38]M. Kaveh and N. Wiser, J. Phys. F (in press).
[39]J. E. Black, Phys. Rev. B 22, 1818 (1980).
[40]M. F. Bishop and A. W. Overhauser, Phys. Rev. B 18, 2447 (1978).
[41]M. L. Cohen and V. Heine, Solid State Physics 24, 37 (1970).
[42]V. Heine and I. Abarenkov, Philos. Mag. 9, 451 (1964).
[43]R. W. Shaw, Phys. Rev. 174, 769 (1968).
[44]P. B. Allen and M. J. G. Lee, Phys. Rev. B 5, 3848 (1972).
[45]N. W. Ashcroft, J. Phys. Chem. 1, 232 (1968).